

# Effect of Monomethyl Itaconate-Grafted HDPE and EPR on the Compatibility and Properties of HDPE–EPR Blends

M. A. López-Manchado,<sup>1</sup> M. Yazdani-Pedram,<sup>2</sup> J. Retuert,<sup>3</sup> R. Quijada<sup>3</sup>

<sup>1</sup>*Instituto de Ciencia y Tecnología de Polímeros, CSIC, Juan de la Cierva, 3 28006-Madrid, Spain*

<sup>2</sup>*Facultad de Ciencias Químicas y Farmacéuticas y Centro para la Investigación Interdisciplinaria Avanzada en Ciencia de los Materiales, Universidad de Chile, Casilla 233, Santiago, Chile*

<sup>3</sup>*Facultad de Ciencias Físicas y Matemáticas y Centro para la Investigación Interdisciplinaria Avanzada en Ciencias de los Materiales, Universidad de Chile, Casilla 2777, Santiago, Chile*

**ABSTRACT:** To improve the compatibility and properties of blends based on high-density polyethylene (HDPE) and the ethylene–propylene copolymer (EPR), the functionalization of both through grafting with an itaconic acid derivative, monomethyl itaconate (MMI), was investigated. The grafting reaction was performed at 180°C in a Brabender Plasticorder using an initial monomer concentration of 3 phr in the case of HDPE and 5 phr in the case of EPR. 2,5-Dimethyl-2,5-bis(*tert*-butylperoxy)hexane was used as a radical initiator for the functionalization of HDPE and dicumyl peroxide was used as a radical initiator for the modification of EPR. The degree of grafting was 1.56% by weight for HDPE and 0.8% by weight for EPR. The effect of grafting on the processability, morphology, and thermal and mechanical

properties of the blends are of particular interest. The results show that the grafting reaction increases the toughness and elongation at break of all tested blends and they retained their strength and stiffness. Moreover, the grafted polymers behaved as nucleating agents, accelerating the HDPE crystallization. These results are particularly relevant when both polymeric phases are modified. Morphological studies are in concordance with the mechanical characterization, showing a reduction of the rubber particle size and a better interfacial adhesion when both polymers are functionalized with MMI.

**Key words:** blends; compatibility; morphology

## INTRODUCTION

Polyolefins, such as polyethylene (PE), are thermoplastics of high consumption because of their well-balanced physical and mechanical properties, good moisture stability, and easy processability at a relatively low cost, which makes them a versatile material with continuously increasing applications. However, in some cases, not all the characteristics of these materials are suitable for common service conditions. So, one of their major drawbacks is their low impact strength, in particular, at low temperatures.<sup>1,2</sup> To overcome these limitations, many studies have been carried out on blends containing polyolefins and elastomers.<sup>3–7</sup> In fact, the toughness of many thermoplastics can be improved by the incorporation of a low-modulus second component. It is assumed that when the rubbery

phase forms highly dispersed small particles it behaves as an effective stress concentrator and enhances resistance to crack propagation in the matrix. In general, polymer blending is a usual practice and relatively of low cost to produce new materials with desired property combinations.

Among different impact modifiers, ethylene–propylene diene terpolymers (EPDM) and ethylene–propylene copolymers (EPR) are the most commonly used and effective ones<sup>8–12</sup> due to their high impact strength over a wide range of temperature. Despite the similarity of the chemical structure of these polymers, the elastomer is not compatible with polyolefins and, as a consequence, the elastomeric phase exists as separate small particles in a continuous thermoplastic matrix.<sup>13,14</sup> Unfavorable interactions at the molecular level give rise to high interfacial tension and impede the melt mixing of the components. Moreover, the incompatibility of these blends cause an unstable morphology and a poor interface adhesion, which are the main causes for poor and undesirable mechanical properties of the blends. To improve the compatibility of these systems, functionalization is often used. Hence, the modification of polymeric materials, in particular, polyolefins, by incorporation of functional monomers with the main objective of obtaining advanced materials with improved technological prop-

Correspondence to: M. A. López-Manchado (lmanchado@ictp.csic.es).

Contract grant sponsors: Ministerio de Ciencia y Tecnología (Spain); Departamento de Investigación y Desarrollo (DID), Universidad de Chile.

Contract grant sponsor: CONICYT; contract grant number: FONDAP 11980002.

TABLE I  
Composition of the Studied HDPE-EPR Blends

HDPE-HDPE-g-MMI-EPR-EPR-g-MMI	HDPE	HDPE-g-MMI	EPR	EPR-g-MMI
100-0-0-0	100	00	00	00
85-0-15-0	85	00	15	00
75-10-15-0	75	10	15	00
85-0-5-10	85	00	5	10
75-10-5-10	75	10	5	10
70-0-30-0	70	00	30	00
60-10-30-0	60	10	30	00
70-0-20-10	70	00	20	10
60-10-20-10	60	10	20	10
50-0-50-0	50	00	50	00
40-10-50-0	40	10	50	00
50-0-40-10	50	00	40	10
40-10-40-10	40	10	40	10
0-0-100-0	00	00	100	00

erties has gained wide industrial applications and has attracted scientific interest during recent years. Several polar monomers, such as oxazoline,<sup>15</sup> mercapto,<sup>16</sup> cyanate ester,<sup>17,18</sup> maleic anhydride,<sup>19-23</sup> and alkyl maleates<sup>24-26</sup> have been investigated. Among them, the most studied modifications of polyolefins are of those with maleic anhydride and alkyl maleates, which are performed in solution, in the solid state, or in the melt phase. In the present study, both high-density polyethylene (HDPE) and the EPR were modified with an itaconic acid derivative, namely, monomethyl itaconate (MMI), in the melt at 190°C, using 2,5-dimethyl-2,5-bis(*tert*-butylperoxy)hexane (Lupersol 101) and dicumyl peroxide, respectively, as radical initiators. The aim of this study was to evaluate the effect of grafting of a polar monomer such as MMI onto HDPE and EPR, via a free-radical reaction, on the compatibility and properties of the blends.

## EXPERIMENTAL

### Materials

HDPE (MFI: 6.7 g min<sup>-1</sup> at 190°C and 2.16 kg, density 0.96 g cm<sup>-3</sup>), kindly supplied by Repsol Química, S.A., under the trade name PE-6006 L and EPR (59% polypropylene content and a Mooney viscosity ML (1+4) at 125°C of 44), generously supplied by EniChem (Milan, Italy), under the trade name Dutral CO 054, were used in this study. Itaconic acid was purchased from Aldrich (Madrid, Spain). MMI was synthesized by esterification of itaconic acid with methanol and the purity was checked by <sup>1</sup>H-NMR spectroscopy. 2,5-Dimethyl-2,5-bis(*tert*-butylperoxy)hexane (Lupersol 101) and dicumyl peroxide were purchased from Akzo (Chicago, IL) and used as radical initiators for HDPE and EPR, respectively.

### Experimental procedures

The grafting reaction of HDPE and EPR with MMI was carried out in a Brabender Plasticorder internal

mixer. The polymer to be grafted was mixed with a predetermined amount of the monomer and the initiator before melt mixing at 190°C. At the end of the reaction, the product was dissolved in hot xylene and then precipitated into acetone. The unreacted monomer, initiator, and possible homopolymer that could eventually form during the grafting reaction were separated from the grafted polymer by exhaustive extraction of the sample with methanol in a Soxhlet for 24 h. The extracted samples were dried under reduced pressure before their analysis. Evidence of grafting as well as its extent, expressed as weight percent of grafting, was obtained by FTIR spectroscopy.

### Blend preparation

HDPE-EPR blends containing 0, 15, 30, 50, and 100% by weight of the elastomer were prepared by melt mixing in a Brabender Plasticorder, equipped with high-shear roller-type rotors. The temperature of the mixing chamber was set to 190°C and the blending time was 10 min. The rotor speed was set to 60 rpm. Immediately after the completion of mixing, the materials were compression-molded for 15 min at 160°C into 0.2-mm-thick plaques before testing. In all cases, the proportion of the grafted polymer was 10% by weight. For each composition, four different blends were analyzed, as shown in Table I. For preparation of the blends without the modified polymer, that is, without using the grafted polymer as a compatibilizer, both polymers were previously passed through the Brabender Plasticorder in the presence of the corresponding peroxide before melt blending.

### Characterization

The evidence of grafting as well as its extent, expressed as weight percent of grafting, was determined by FTIR spectroscopy. FTIR spectra were recorded on a Bruker IFS-28 spectrometer from 4000 to 400 cm<sup>-1</sup>.

Films of 600- $\mu\text{m}$  thickness from the unmodified polymers and the grafted samples were obtained by compression molding between steel plates covered with thin aluminum sheets at 190°C for 1 min.

The rheological measurements were performed using a Rheometrics mechanical spectrometer, RMS, Model 605, with parallel-plate geometry. Tests were carried out in dynamic frequency modes at 190°C. Dynamic shear properties were determined as a function of the angular frequency in the range 0.1–500 rad/s. The amplitude strain was maintained constant at 5%.

Dynamic mechanical properties of the solid polymer were determined using a Metravib dynamic mechanical thermoanalyzer, Model Mark 03. The nominal dimensions of the specimens were  $25 \times 10 \times 6$  mm. Tests were carried out in the torsion deformation mode, at a frequency of 5 Hz, and the temperature programs were run from  $-140$  to  $40^\circ\text{C}$ , at a heating rate of  $2^\circ\text{C}/\text{min}$ , under a controlled sinusoidal strain in a flow of nitrogen.

Thermal analysis experiments were performed using a Mettler Toledo differential scanning calorimeter, Model DSC 822. Crystallization tests were carried out in isothermal conditions at  $123^\circ\text{C}$ . Samples of about 8 mg were melted at  $200^\circ\text{C}$  for 10 min, to eliminate any previous thermal history in the material. Then, they were rapidly cooled to the crystallization temperature,  $T_c$  (in our case,  $123^\circ\text{C}$ ), and maintained at that temperature for the necessary time to complete the crystallization of the matrix. The experiments were carried out in a nitrogen atmosphere, and after the isothermal crystallization tests, a dynamic scan at  $10^\circ\text{C}/\text{min}$  was performed to check the presence of the residual crystallinity. Plots of the degree of crystallization as a function of time were made by integrating the area under the exothermic peaks. Subsequently, the melting temperature ( $T_m$ ) of the materials was considered to correspond to the maximum of the endothermic peak.

Thermal degradation measurements were performed using a Mettler Toledo thermogravimetric analyzer (TGA), Model SDTA 851. Temperature programs were run from  $30$  to  $600^\circ\text{C}$  at a heating rate of  $10^\circ\text{C}/\text{min}$ . A nitrogen flow ( $20$  mL/min) was used to remove all corrosive gases involved in the degradation and to avoid thermoxidative degradation.

Mechanical characterization was also carried out by tensile testing and impact measurements. Tensile testing was performed at room temperature on an Instron dynamometer, Model 4301, according to ASTM D 638M. Tests were carried out at a crosshead speed of  $5$  mm/min until a deformation of 20% and then at speed of  $50$  mm/min at break. Impact experiments were carried out according to ASTM D-256 (V-notched) at room temperature, in an Izod pendulum Ceast Model Resil 25, with an impact speed of  $3.48$  ms $^{-1}$ , recording

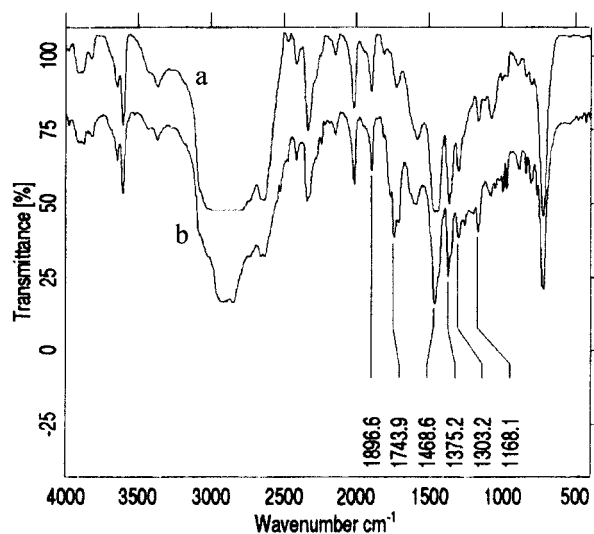


**Figure 1** FTIR spectrum of (a) HDPE and (b) MMI-grafted HDPE.

the maximum force and the energy to fracture. The notches were prepared in a Ceast electrical notching apparatus at 20% of the thickness and the angle of the "V" side grooves was  $45^\circ$ . All mechanical properties were the average of at least seven measurements.

The blends' morphology was characterized by scanning electron microscopy (SEM) using a Tesla BS 343 A scanning electron microscope. Micrographs were obtained after extraction of the EPR phase from the surface of cryogenically fractured samples using toluene at  $70^\circ\text{C}$  for 8 h. Fracture surfaces of the test specimens were sputtered with gold before being observed in the SEM.

## RESULTS AND DISCUSSION

### Evidence of grafting

The existence of grafted MMI in HDPE as well as EPR was confirmed by FTIR spectroscopy. Figure 1 shows the FTIR spectra of HDPE and HDPE grafted with MMI (HDPE-g-MMI). The absorption band observed at  $1744$  cm $^{-1}$  is due to the carboxyl group of the ester linkage of MMI and confirms the incorporation of this monomer in the HDPE chains. The intensity of this band was compared with that of the methylene group deformation from HDPE centered at  $1468$  cm $^{-1}$ . The  $1744/1468$  cm $^{-1}$  band ratio was defined as the carbonyl index ( $I_c$ ). This can be considered as a measure of the extent of grafting of the monomer in HDPE either as single units and or as poly(MMI) chains. The extent of grafting was converted into the incorporated weight percent ( $G_{\text{MMI}}$  in weight percent) of the monomer using a calibration curve obtained from the FTIR analysis of the physical mixtures of HDPE with different amounts of MMI. These mixtures were obtained

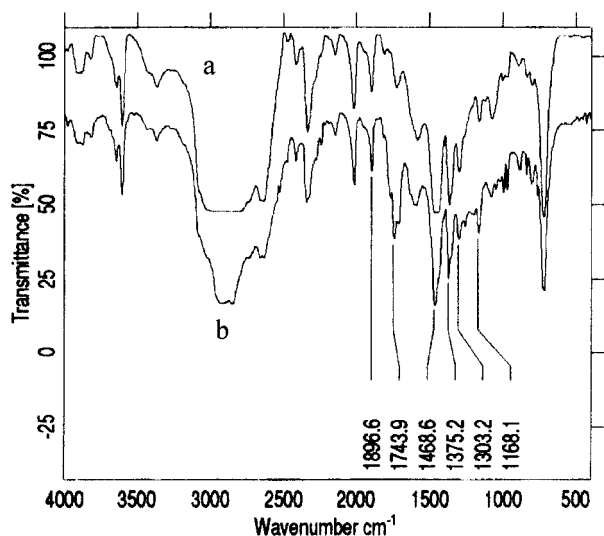


Figure 2 FTIR spectrum of (a) EPR and (b) MMI-grafted EPR.

by the melt mixing of HDPE and MMI in a Brabender mixing chamber at 190°C under a nitrogen stream for 6 min. The percentage of grafting can be calculated using the relation

$$G_{\text{MMI}} \text{ in wt\%} = I_c / 0.6764 \quad (1)$$

A degree of grafting of 1.56% by weight for HDPE was obtained.

Similarly, in the case of EPR grafted with MMI (EPR-g-MMI) (Fig. 2), the intensity of the carbonyl absorption band from the grafted MMI at 1739  $\text{cm}^{-1}$  was compared with both the methyl group from polypropylene centered at 1167  $\text{cm}^{-1}$  and that of methylene groups at 1460  $\text{cm}^{-1}$  from polyethylene, considering that EPR is a random copolymer of ethylene-*co*-propylene. The 1739/1460  $\text{cm}^{-1}$  + 1167  $\text{cm}^{-1}$  band ratio was defined as the carbonyl index ( $I_c$ ). A calibration curve was also constructed in this case as was described for the HDPE. The percentage of grafting of MMI onto EPR can be estimated by using the relation

$$G_{\text{MMI}} \text{ in wt\%} = I_c / 0.7602 \quad (2)$$

A degree of grafting of 0.8% by weight for EPR was obtained.

### Rheological properties

The flow properties of the materials studied in the molten state were analyzed by rheological studies. The variation of the complex viscosity ( $\eta^*$ ) as a function of the angular frequency, for HDPE–EPR blends at different compositions, is shown in Figure 3. It can be easily observed that the complex viscosity of all the

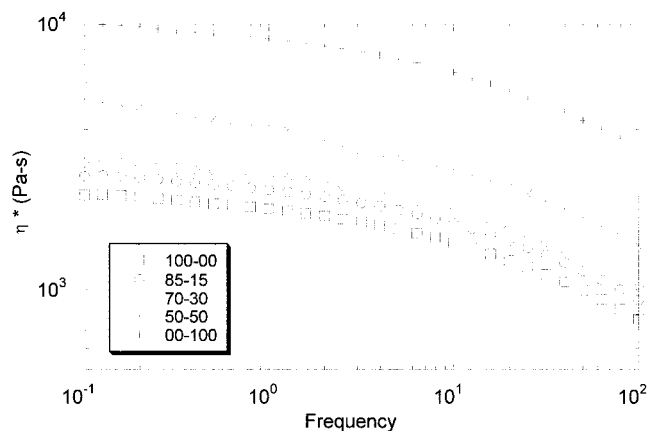


Figure 3 Variation of complex viscosity with angular frequency at 180°C for different HDPE–EPR blends.

samples gradually decreases with an increasing angular frequency, showing the pseudoplastic nature of these materials (shear thinning). It is well known that the viscosity of the blends lies, in general, between the viscosity of the components from which they are produced. So, from Figure 3, it can be seen that the viscosity of HDPE increases by increasing the amount of the elastomer in the blend and that the viscosity of the blends is between that of their constituents.

To evaluate the effects of the grafting reaction of both polymers with MMI on the rheological properties of the blend, the variation of the viscosity for unmodified and modified HDPE–EPR (85–15) blends are presented in Figure 4. It is observed that the viscosity of the blend containing small amounts of functionalized polymers increases as compared to that of the unmodified blends, revealing their higher viscosity at a particular angular frequency. Moreover, this effect is larger when both polymeric phases are modified. The higher viscosity of this blend indicates strong interactions between the blend components. In addition, the

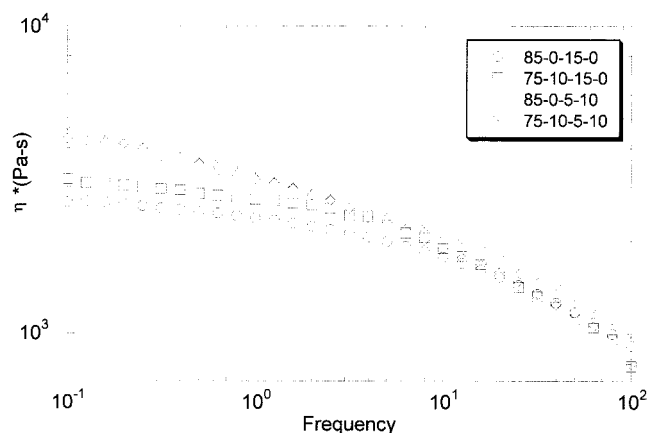


Figure 4 Variation of complex viscosity with angular frequency at 180°C for unmodified and MMI-functionalized HDPE–EPR (85–15) blends.

TABLE II  
Dynamic Mechanical Analysis for Unmodified and MMI-functionalized HDPE–EPR (50–50) Blends

HDPE–HDPE-g-MMI–EPR–EPR-g-MMI	HDPE			EPR		
	Tan $\delta$	$T_g$ (°C)	$G'$ (MPa)	Tan $\delta$	$T_g$ (°C)	$G'$ (MPa)
50–0–50–0	0.040	–120.1	$2.63 \times 10^9$	0.064	–37.2	$9.52 \times 10^8$
40–10–50–0	0.044	–118.6	$2.17 \times 10^9$	0.067	–36.7	$9.11 \times 10^8$
50–0–40–10	0.048	–116.5	$1.86 \times 10^9$	0.080	–35.8	$8.78 \times 10^8$
40–10–40–10	0.049	–115.3	$1.79 \times 10^9$	0.087	–38.2	$7.49 \times 10^8$

effect of the grafted polymers in increasing the viscosity of the HDPE–EPR blends is more marked in the low angular frequency region, that is, the viscosity of the blend at the high angular frequency region hardly varies with the grafted polymers' addition. It must be pointed out that the higher viscosity of the functionalized blends cannot be attributed to the formation of cyclic anhydride by changes in the structure of the grafted ester groups at high temperatures during the rheological characterization performed in this research. This was verified by FTIR spectroscopy, in which the peak corresponding to the carboxyl group of the ester linkage does not vary during the rheological analysis. The variation of the viscosity can be explained in terms that the compatibilizer located at the interface decreases the interfacial tension and highly favors intermixing, and, consequently, an increase of the viscosity is expected. Similar results were reported by Willis and Favis<sup>27</sup> and George et al.<sup>28,29</sup> when analyzing the viscosity of binary polymer blends upon the addition of a compatibilizer. The authors reported that the viscosity of a polymer blend depends on different factors such as the miscibility of the system, morphology, interfacial adhesion, and interface layer thickness (compatible domain). Therefore, the compatibilizer located in the interface will induce an increase in interfacial thickness and, consequently, an effective stress transfer between the dispersed phase and the continuous phase, and an increase in interfa-

cial adhesion is obtained. This will give rise to a reduction in interlayer slip and, consequently, to an increase in the viscosity.

### Dynamic mechanical analysis

The dynamic mechanical properties of HDPE–EPR blends were studied over a wide temperature range (–140 to 40°C) and the results are reported in Table II. Figure 5 shows the storage modulus of the HDPE/EPR blends at different rubber contents. It is observed that by increasing the elastomer percentage in the blend the storage modulus decreases, which is correlated with the elastomer function as the impact modifier of the polyolefin matrix. As reported in Table II, all the blends show two glass transition temperatures, corresponding to those of the pure homopolymers. The first one is detected approximately at –120°C, corresponding to the glass transition temperature ( $\alpha$ -relaxation) of the amorphous regions of the HDPE component. Another loss-peak maximum is in the neighborhood of –35°C, assigned to the glass transition temperature ( $\alpha$ -relaxation) of the rubbery phase. These results indicate the formation of a two-phase system with a very limited degree of miscibility of their components. Figure 6 shows the tan  $\delta$  traces of unmodified and modified HDPE–EPR (50–50) blends. It can be seen that the grafting reaction gives rise to an increase of the height of the tan  $\delta$  traces, which is

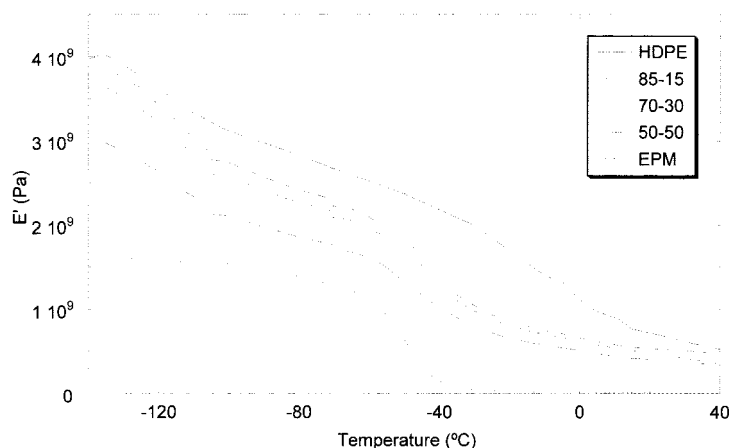
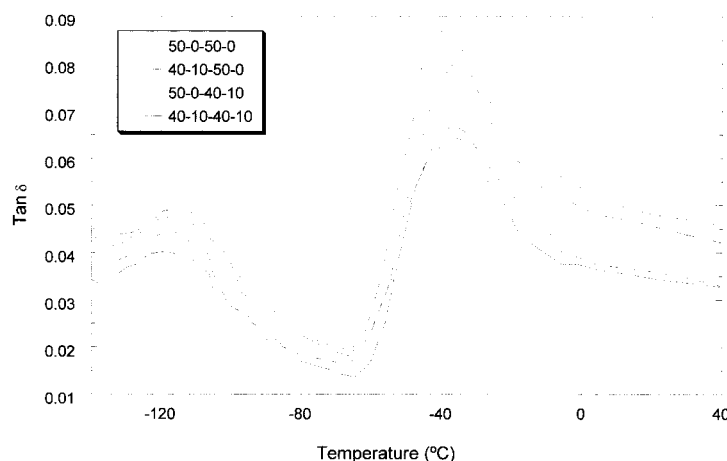


Figure 5 Storage modulus of HDPE–EPR blends with different rubber content.



**Figure 6** Tan  $\delta$  traces of unmodified and MMI-functionalized HDPE-EPR (50-50) blends.

related to a better behavior as an impact modifier. On the other hand, the peak corresponding to the glass transition temperature of HDPE is shifted to higher temperatures (about 5°C) with the grafted polymers. According to these results, it can be assumed that the incorporation of MMI groups restricts the segmental mobility of HDPE chains, probably due to a better interfacial adhesion between both polymeric matrices. It is of interest to note that these effects are more significant in those blends containing both modified polymers. These results are in concordance with the rheological analysis discussed above. In turn, the glass transition temperature of the elastomer hardly varies with the functionalized polymers.

### Crystallization kinetics

The effects of the incorporation of small amounts of grafted polymers into the blend, on the crystallization of HDPE, was also analyzed by differential scanning calorimetry (DSC). For this purpose, isothermal crystallization tests were performed at 123°C and the results are summarized in Table III. It can be deduced that the crystallization rate of HDPE increases in the presence of the rubbery phase, this increment being

more evident at a lower concentration of the amorphous polymer (to 30%). This behavior is clearly reflected by analyzing the half-time of crystallization, where a considerable decrease is observed in the presence of the elastomeric phase. This nucleating effect can be attributed to the modification of the matrix structure. Thus, a change of the average size and number of the spherulites is induced and the structural changes are very important to interpret the function of the elastomer as an impact modifier of the polyolefin matrix. It can be assumed that the elastomer behaves as an effective nucleating agent of the HDPE matrix. However, at higher percentages of EPR in the blend (50%), an inversion of the crystallization rate increase is observed. This particular behavior suggests that, although the elastomer acts as a nucleating agent, the same rubber phase at high percentages in the blend could be responsible for an impingement effect on the spherulitic growth. In addition, the incorporation of MMI groups into the matrix increases the crystallization rate of HDPE, as can be deduced from Table III, that is, a considerable decrease of the half-time of crystallization of HDPE is observed with an increasing percentage of MMI-grafted HDPE in the blend. This could be accounted for by an increase of the hetero-

**TABLE III**  
Crystallization Parameters for HDPE-EPR Blends with Different Rubber Content and Unmodified and MMI-functionalized HDPE-EPR(85-15) Blend

HDPE-HDPEg-MMI-EPR-EPRg-MMI	$n$	$K_n$ ( $\text{min}^{-1}$ )	$\tau_{1/2}$ (s)	$T_m$ (°C)	$\Delta H_c$ (g/mol)
100-0-0-0	2.10	$3.10 \times 10^{-1}$	116.2	138.8	183.9
90-10-0-0	2.12	$2.24 \times 10^{-1}$	102.1	139.3	202.7
80-20-0-0	2.14	$2.40 \times 10^{-1}$	98.4	138.2	216.1
70-30-0-0	2.10	$2.61 \times 10^{-1}$	95.6	137.9	223.4
85-0-15-0	2.07	$2.05 \times 10^{-1}$	108.0	138.0	181.1
75-10-15-0	2.16	$3.02 \times 10^{-1}$	88.2	135.3	179.2
85-0-5-10	2.16	$3.53 \times 10^{-1}$	82.0	136.7	233.8
75-10-5-10	2.01	$3.90 \times 10^{-1}$	79.8	136.6	229.7
70-0-30-0	2.19	$8.06 \times 10^{-1}$	66.0	133.6	132.4
50-0-50-0	2.09	$1.84 \times 10^{-1}$	112.9	132.7	85.1

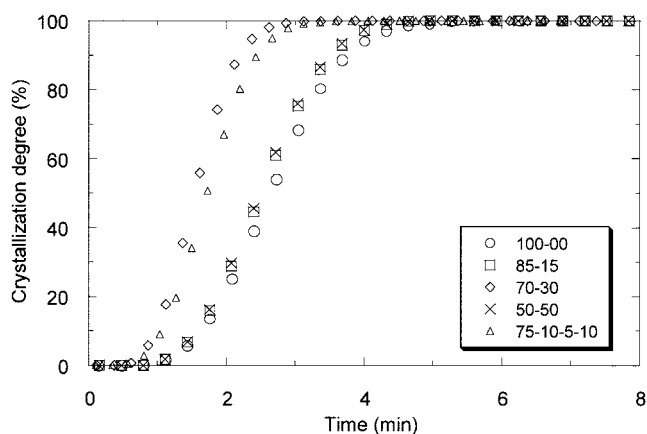


**Figure 7** Degree of crystallization of HDPE-EPR blends with different rubber content and the HDPE-HDPE-g-MMI-EPR-EPR-g-MMI (75-10-5-10) blend at 123°C.

geneous nuclei due to the mixing, that is, as a consequence of the migration of active nuclei between the molten components.<sup>30</sup>

Figure 7 shows the degree of crystallization as a function of time for the unmodified HDPE-EPR blends at different compositions and the MMI-functionalized HDPE-EPR (85-15) blend. It can be observed that the crystallization rates of the modified blends are higher than those of the unmodified blends, which is reflected in a considerable decrease of the half-time of crystallization as shown in Table III. This behavior is particularly evident for the blend containing both grafted polymers. It can be assumed that the functional polar monomer used in this work behaves as an effective nucleating agent for the HDPE matrix, promoting the crystallization of the semicrystalline polymer. These results can be explained by the fact that a higher number of active nuclei are formed during the crystallization process. Moreover, an increase in the crystallinity of HDPE is observed for the blends with the grafted polymer. Jafari and Gupta<sup>31</sup> demonstrated that the crystallinity is intimately related to the segmental mobility of the HDPE chain and, then, the glass transition temperature of HDPE is shifted to higher temperatures. These results are in line with those obtained by dynamic mechanical analysis (DMA), where an increase of the  $T_g$  of HDPE was observed. Furthermore, no significant changes in the melting point of the HDPE phase was detected in the blends.

### Thermogravimetric analysis

The results of the thermogravimetric analysis performed on the pure HDPE and the functionalized and nonfunctionalized HDPE-EPR (70-30) blends at 10°C/min, under a nitrogen stream, are reported in terms of the percentage of weight loss as a function of

the temperature in Figure 8. A single peak on the degradation curve is observed. Although miscible blends produce a single degradation pattern, the opposite deduction is not necessarily true. In our case, the partial immiscibility of HDPE and EPR has already been demonstrated by microscopy analysis and by the presence of two glass transition temperatures obtained by DMA. Thus, the single degradation peak of this mixture must be associated to similar degradation reactions of these polymers with a similar chemical structure. Moreover, a slight displacement of the degradation curve to upper temperatures is observed when functionalized polymers with MMI are added to the blends. No significant differences were observed independent of which modified matrix was used. These results support the assumption that the presence of functionalized polymers improves the adhesion between both matrices, giving rise to a more thermally stable material.

### Mechanical characterization

The mechanical properties of the HDPE-EPR blends were also analyzed by tensile and impact measurements. As was expected, the mechanical characterization shows a strong influence of the composition on the properties studied (Table IV). Therefore, the modulus and the tensile strength decrease with an increasing EPR content in the blend. In addition, the impact strength increases as the percentage of EPR in the blend increases, indicating the function of EPR as impact modifier of polyolefin. This fact can be explained in terms that the rubbery phase is highly deformed during the impact test and, thus, absorbs a part of the impact energy. The rubber domains deformed because the shear yield, which is considered to be the main mechanism of impact toughness of polyolefin-elastomer blends at the service temperature.<sup>32-34</sup>

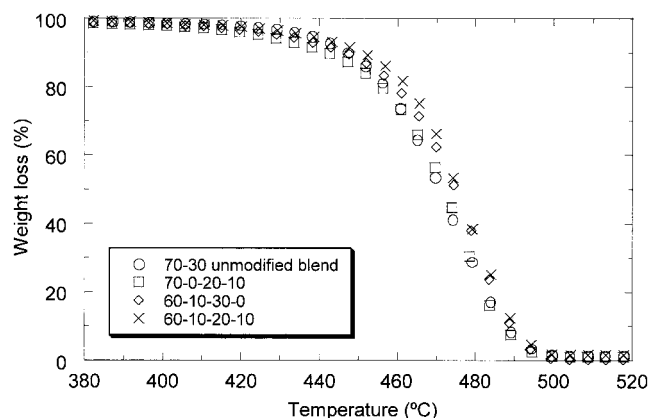


**Figure 8** Weight loss of unmodified and MMI-functionalized HDPE-EPR (70-30) blends as a function of temperature.

TABLE IV  
Mechanical Properties of HDPE-EPR Blends

HDPE-HDPE-g-MMI-EPR-EPR-g-MMI	Young's modulus (MPa)	Maximum strength (MPa)	Deformation at break (%)	Impact strength (kJ/m <sup>2</sup> )
100-0-0-0	868	22.0	608	25
85-0-15-0	619	16.7	428	45
75-15-15-0	611	16.5	483	48
85-0-5-10	625	16.3	686	57
75-10-5-10	634	16.3	769	58
70-0-30-0	431	12.2	408	80
60-10-30-0	417	11.5	452	86
70-0-20-10	429	10.4	656	105
60-10-20-10	444	12.6	693	108
50-0-50-0	213	7.1	578	150
40-10-50-0	206	6.8	630	151
50-0-40-10	217	6.8	835	183
40-10-40-10	227	6.8	871	184
0-0-100-0	4.5	1.8	562	—

It is of interest to point out that the blends containing grafted polymers show a higher toughness without any reduction of the strength and stiffness. Moreover, a marked increase of the deformation at break of the material is observed. Generally, about 80% increments are observed when grafted polymers are added to the blends. This behavior is particularly evident when both polymeric phases are modified with MMI. An explanation of these results can be found in terms that the compatibilization by MMI-modified polymers improves the interfacial adhesion between the both polymeric phases as well as the size reduction of the rubber particles in the continuous HDPE matrix. It is assumed that a decrease of the rubber particle size is related to enhancement of the impact strength of the material. It can be concluded that in the presence of the compatibilizer a better balance among all tested properties was obtained.

### Morphological analysis

The fracture surface of the blends after extraction of the EPR phase using toluene at 70°C was analyzed using SEM. Figure 9 shows micrographs of unmodified and modified HDPE-EPR (85-15) blends at the same magnification. As is evident from the scanning electron micrographs, the small rubber particles are uniformly distributed in the polypropylene matrix. In addition, the micrographs show that the rubber domains in the blends containing grafted polymers are much more well distributed and more regular than are the unmodified blends, which improves the adhesion between both polymeric phases. Moreover, the size of the rubber particles is decreased when the grafted polymers are added to the blend, in particular, in blends containing both functionalized polymers, this being one of the aspects responsible for the better impact behavior. Bedia et al.<sup>35</sup> demonstrated that, as

the EPR content increases, the rubber domain dispersed in the continuous matrix increases, this effect being particularly evident at concentrations above 40% of EPR in the blend. On the other hand, they observed that the highest impact strength was obtained at 40% EPR and starts to decrease for higher concentrations. It is well assumed that the size of the rubber particles is intimately related to their function as impact modifiers for polyolefins, that is, a decrease of the rubber particles' size is correlated with enhancement of the impact strength of the material.

### CONCLUSIONS

The use of MMI-grafted HDPE and EPR on the compatibility and properties of the blends was studied. The grafting reaction was confirmed by FTIR spectroscopy, where a degree of grafting of 1.56% by weight for HDPE and 0.8% by weight for EPR was determined. The melt viscosities of the polymers (HDPE and EPR) and the blends decrease as the frequency increases, showing pseudoplastic behavior. In addition, the blend viscosity was increased in the presence of the grafted polymers. On the other hand, the addition of the grafted polymers considerably improved the deformation at break and impact strength as compared with the unmodified blends, without hardly varying their strength and stiffness. These results were corroborated by SEM observations, where a more stable morphology was observed in the blends containing grafted polymers. The addition of grafted HDPE and EPR with MMI to blends decreases the rubber particle size and, thus, a finer dispersion of the elastomeric phase as small droplets, well embedded in the HDPE matrix, was observed. This statement was particularly evident when both grafted polymers were added to the blend. This could probably be due to the interaction between the itaconate groups of both poly-



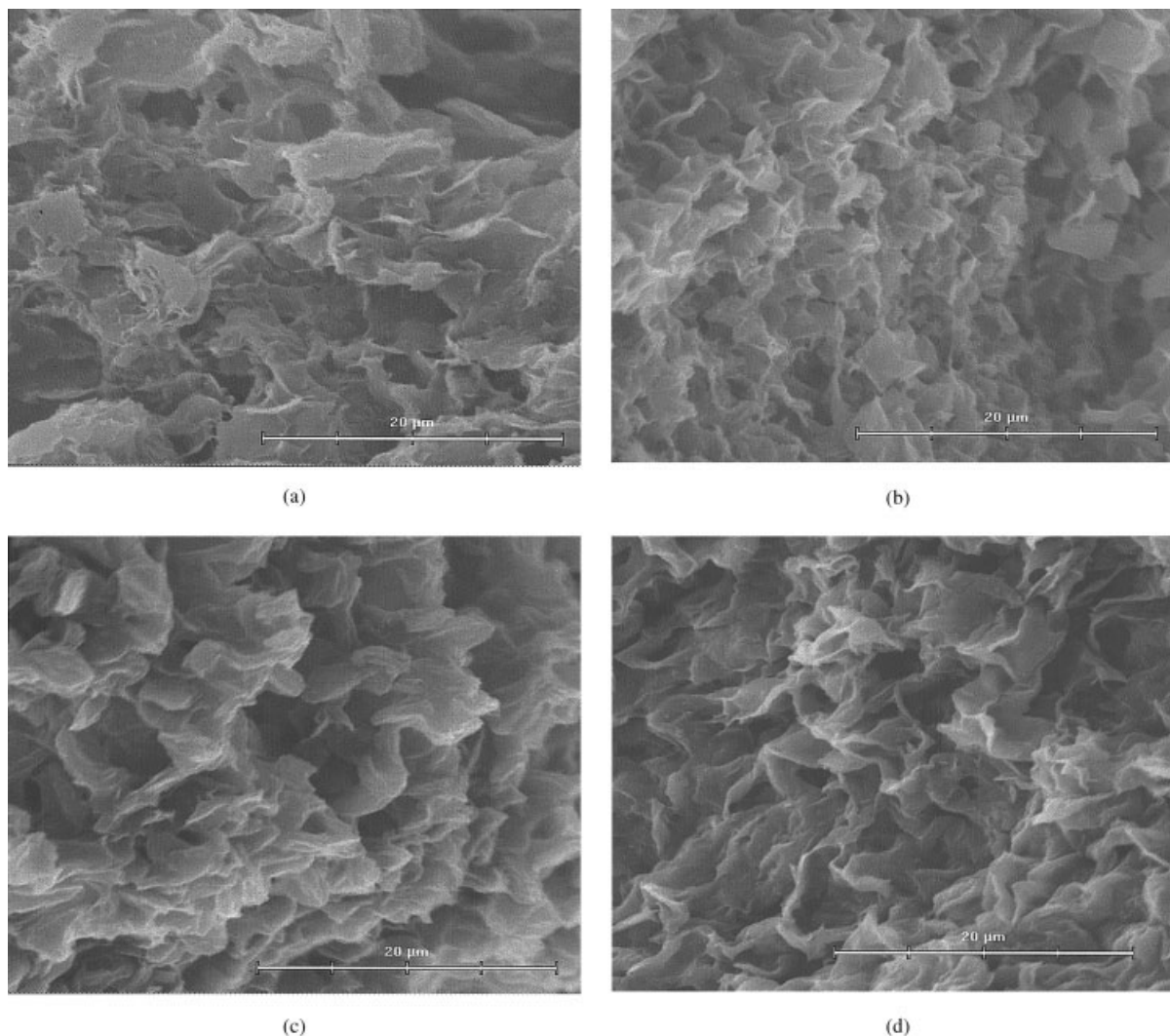


**Figure 9** SEM micrographs of HDPE-EPR (85-15) blend: (a) unmodified blend; (b) HDPE-HDPE-g-MMI-EPR (75-10-15-0) blend; (c) HDPE-EPR-EPR-g-MMI (85-0-5-10) blend; (d) HDPE-HDPE-g-MMI-EPR-EPR-g-MMI (75-10-5-10) blend.

meric phases. This study demonstrated that MMI-grafted HDPE and EPR behave as effective compatibilizers in blends based on polyolefins and thermoplastic elastomers.

The authors acknowledge the financial support of the Ministerio de Ciencia y Tecnología (Spain) for the concession of a Ramón y Cajal contract to one of the authors (M. A. L.) and of CONICYT, Project FONDAP 11980002 and of the Departamento de Investigación y Desarrollo (DID), Universidad de Chile.

## References

1. Rader, C. P. In *Handbook of Thermoplastic Elastomers*, 2nd ed.; Walker, B. M.; Rader, C. P., Eds.; Van Nostrand Reinhold: New York, 1988; Chapter 2.
2. Thomas, D. A.; Sperling, L. K. In *Polymer Blends*; Newman, S.; Paul, D. R., Eds.; Academic: New York, 1978; Vol. 2.
3. Martuscelli, E.; Silvestre, C.; Abate, G. *Polymer* 1992, 23, 23.
4. Danesi, C.; Porter, R. S.; Ragosta, G. *Mater Sci* 1989, 21, 1775.
5. Karger-Kocsis, J. *J Appl Polym Sci* 1972, 16, 2375.
6. Gupta, A. K.; Srinivasan, K. R.; Krishna Kumar, P. *J Appl Polym Sci* 1991, 44, 4415.
7. Gupta, A. K.; Ratnan, B. K.; Srinivasan, K. R. *J Appl Polym Sci* 1992, 45, 1303.
8. Walker, B. M. In *Handbook of Thermoplastic Elastomers*; Van Nostrand Reinhold: New York, 1979.
9. Whelan, A.; Lee, K. S. In *Developments in Rubber Technology 3. Thermoplastic Rubbers*; Whelan, A.; Lee, K. S., Eds.; Applied Science: London, 1982.
10. Thomas, S.; George, A. *Eur Polym J* 1992, 28, 1451.
11. López Manchado, M. A.; Biagiotti, J.; Arroyo, M.; Kenny, J. M. *Macromol Symp* 1999, 148, 345-360.
12. Campbell, D. S.; Elliot, D. S.; Wheelan, M. A. *Nat Rubber Technol* 1978, 1, 21.
13. Yang, D.; Zhang, B.; Yang, Y.; Fang, Z.; Sun, G.; Feng, Z. *Polym Eng Sci* 1984, 24, 612.
14. Lee, B. L. U.S. Patent 4 975 207, 1990.
15. Vocke, C.; Anttila, U.; Heino, M.; Hietaoja, P.; Seppälä, J. *J Appl Polym Sci* 1998, 70, 1923.
16. Oliveira, M. G.; Soanes, B. G.; Santos, C. M.; Diniz, M. F.; Dutra, R. C. *Macromol Rapid Comm* 1999, 10, 526.
17. Hillermeier, R. W.; Seferis, J. C. *J Appl Polym Sci* 2000, 77, 556.

18. Ciardelli, F.; Aggietto, M.; Passaglia, E.; Ruggeri, G. *Macromol Symp* 1998, 129, 79.
19. Gaylord, N.; Mehta, M. *J Polym Sci Pol Lett* 1982, 20, 481.
20. Gaylord, N.; Mehta, M.; Mehta, R. *J Appl Polym Sci* 1987, 33, 2549.
21. Ganzeveld, K.; Janssen L. P. *Polym Eng Sci* 1992, 32, 467.
22. Benedetti, E.; D'Alessio, A.; Aglietto, M.; Ruggeri, G.; Vergamini, P.; Ciardelli, F. *Polym Eng Sci* 1986, 26, 9.
23. Machado, A. V.; Duin, M.; Covas, J. A. *J Appl Polym Sci* 2000, 38, 3919.
24. Greco, R.; Maglio, G.; Musto, P. V. *J Appl Polym Sci* 1987, 33, 2513.
25. Xie, H.; Feng, D.; Guo J. *J Appl Polym Sci* 1997, 64, 329.
26. Blanca Rojas, G.; Fatou, J. G.; Carmen Martínez, M. A.; Laguna, O. *Eur Polym J* 1997, 33, 725.
27. Willis, J. M.; Favis, B. D. *Polym Eng Sci* 1998, 28, 1416.
28. George, J.; Ramamurthy, K.; Anand, J. S.; Groeninckx, G.; Varughese, K. T.; Thomas, S. *Polymer* 1999, 40, 4325.
29. George, J.; Ramamurthy, K.; Varughese, K. T.; Thomas, S. *J Appl Polym Sci* 2000, 38, 1104.
30. Bartczak, Z.; Galeski, A.; Pracella, M. *Polymer* 1986, 27, 537.
31. Jafari, S. H.; Gupta, A. K. *J Appl Polym Sci* 2000, 78, 962.
32. Newman, S. *Polym Plast Technol Eng* 1973, 2, 67.
33. Sultan, J. N.; Liable, R. C.; Magarry, F. *J Appl Polym Sci* 1971, 16, 127.
34. Petrich, R. P. *Polym Eng Sci* 1977, 12, 757.
35. Bedia, E. L.; Astrini, N.; Sudarisman, A.; Sumera, F.; Kashiro, Y. *J Appl Polym Sci* 2000, 78, 1200.